Hydrothermal stability of yttria- and ceria-doped tetragonal zirconia–alumina composites

MASANORI HIRANO, HIROSHI INADA
Noritake Co. Ltd, Noritake, Nishi-ku, Nagoya-shi, Japan

Changes in the crystalline phase and microstructure resulting from hydrothermal ageing of Y-TZP, (Y,Ce)-TZP, Y-TZP–Al_2O_3 composites and (Y,Ce)-TZP–Al_2O_3 composites were investigated under hydrothermal conditions at 180 °C and 1 MPa. Although (Y,Ce)-TZP showed no tetragonal-to-monoclinic (t→m) phase transformation during low-temperature ageing in air as compared with 3Y-TZP, the tetragonal phase of (Y,Ce)-TZP easily transformed to monoclinic phase by ageing under hydrothermal condition. This t → m phase transformation invaded the inside of the body accompanied by microcracks. (Y,Ce)-TZP–Al_2O_3 composites were resistant to phase transformation during hydrothermal ageing.

1. Introduction

It is well known that Y-TZP exhibits high fracture strength and toughness [1, 2]. This improvement in strength and toughness has been explained as due to a stress-induced phase transformation of tetragonal zirconia precipitates to the stable monoclinic form [1, 2]. Zirconia ceramics have hitherto received special attention due to their excellent mechanical properties. However, as first reported by Kobayashi *et al.* [4], the fracture toughness and strength of Y-TZP are greatly degraded by low-temperature ageing at 200 to 400 °C in air. The loss of strength and toughness by low-temperature ageing is believed to be caused by tetragonal-to-monoclinic (t → m) phase transformation on the surface of sintered materials. This degradation accompanied by the t → m phase transformation of Y-TZP by low-temperature ageing occurs with a high rate and at a lower temperature in a wet atmosphere than the case in a dry atmosphere [5]. A number of studies concerning this ageing phenomenon have been conducted to eliminate the degradation in mechanical properties [6, 7]. Tsukuma [8] reported that Ce-TZP (12 mol %) showed resistance to phase transformation during low-temperature ageing in air. It has also been reported that the t → m phase transformation in Y-TZP during low-temperature ageing was fully controlled by doping with ceria [9]. Although Ce-TZP and ceria-doped Y-TZP have resistance to phase transformation during low-temperature ageing, their fracture strengths are modest and are lower than that of Y-TZP [10]. Lange [11] reported that improved strength and toughness could be achieved for ceramics containing tetragonal ZrO_2 and α-Al_2O_3. We fabricated (Y,Ce)-TZP–Al_2O_3 composites using fine powders of Y_2O_3-CeO_2-ZrO_2 prepared by hydrolysis of $ZrOCl_2$ solution [12].

In the present study, the phase transformation and changes in microstructure of (Y,Ce)-TZP–Al_2O_3 composites as compared with 3Y-TZP. (Y,Ce)-TZP and 3Y-TZP–Al_2O_3 composites were investigated. The stability of the tetragonal phase in (Y,Ce)-TZP–Al_2O_3 composites under hydrothermal conditions at 180 °C and 1 MPa was evaluated.

2. Experimental procedure

As shown in Table I, the fine powders with compositions 4 mol % $YO_{1.5}$–4 mol % CeO_2–ZrO_2, 2.5 mol % $YO_{1.5}$–4 mol % CeO_2–ZrO_2, and 3 mol % Y_2O_3– ZrO_2 were prepared by the hydrolysis technique using an aqueous solution of $ZrOCl_2$, YCl_3, and $CeCl_3$. The starting materials were as-synthesized (Y,Ce)-TZP and Y-TZP powder and Al_2O_3 powder. The Al_2O_3 powder used (TMD, Taimei Chemical Industry Co., Nagano, Japan) had a particle size of 0.2 μm and a purity of 99.99%. The TZP and Al_2O_3 powders were mixed by ball-milling with zirconia balls, followed by drying in air. The powders were uniaxially pressed at 19.6 MPa to form plates, and then isostatically cold-pressed at 196 MPa. The green compacts were either sintered at 1500 to 1550 °C for 2 h in air or pre-sintered to closed porosity at 1350 to 1400 °C for 2 h and hot isostatically pressed at 1400 °C for 30 min at 147 MPa in Ar gas. The bulk density of the sintered bodies was measured by the Archimedes technique. The average grain size was determined by the intercept method. Fracture strength was measured

TABLE I Composition of zirconia powders employed in this study

Material	Composition
3Y-TZP	$3Y_2O_3 \cdot 97ZrO_2$
(2.5Y,4Ce)-TZP	$2.5YO_{1.5} \cdot 4CeO_2 \cdot 93.5ZrO_2$
(4Y,4Ce)-TZP	$4YO_{1.5} \cdot 4CeO_2 \cdot 92ZrO_2$

by carrying out three-point bending tests at a span of 30 mm and a crosshead speed of 0.5 mm min^{-1}, using an Instron testing machine with sample pieces measuring 3 mm × 4 mm × 40 mm. The tensile surface was finished with a 140 grit diamond wheel with the grinding passes to parallel to the tensile axis. Modulus of elasticity was determined by stress–strain curves measured by using the Instron testing instruments. The specimens ground using a 140 grit diamond wheel were aged at 250 °C in air and under hydrothermal condition at 180 °C and 1 MPa. The autoclave cycle for the hydrothermal ageing test is shown in Fig. 1. The ageing time was estimated as the total holding time at 180 °C and 1 MPa. The phases were identified by X-ray diffraction analysis on the plate surface. Scans of 2θ between 27 and 33° were conducted to estimate the monoclinic to (tetragonal + cubic) zirconia ratio [13]. Microstructures of the surface and cut surface of aged specimens were observed by SEM.

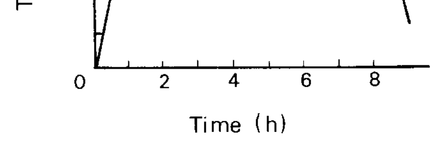

Figure 1 Autoclave cycle.

3. Results and discussion

3.1. Characterization of as-sintered materials

The bulk density, grain size of zirconia, bending strength, and elastic modulus of the sintered materials are summarized in Table II. The densities of 3Y-TZP, (4Y,4Ce)-TZP and (2.5Y,4Ce)-TZP were 99.7, 98.9 and 98.4% of theoretical density, respectively. The theoretical density of (Y,Ce)-TZP was determined from the lattice parameters using the equations [14]

$$\begin{aligned} a\,(\text{nm}) &= 0.000251\text{Y} + 0.000332\text{Ce} + 0.50856 \\ c\,(\text{nm}) &= -\,0.000249\text{Y} + 0.000255\text{Ce} \\ &\quad + 0.51897 \end{aligned} \tag{1}$$

where a and c are for the unit cell of cubic ZrO_2, Y and Ce are the mole percentages of $YO_{1.5}$ and CeO_2, respectively; $a = 2^{1/2}a_t$ and $c = c_t$ where a_t and c_t are for the unit cell of tetragonal ZrO_2. The sinterability of (Y,Ce)-TZP was not so good as that of Y-TZP. The density of (4Y,4Ce)-TZP–Al_2O_3 composites was 99.6% of theoretical density and hot isostatically pressed samples were nearly 100% dense. The microstructure of each sintered body was composed of a uniform grain size as listed in Table II. The fracture strength of (4Y,4Ce)-TZP was 840 MPa and it was lower than that of 3Y-TZP. Composites consisting of (4Y,4Ce)-TZP and 25 wt % Al_2O_3 fabricated by normal sintering showed about the same strength as 3Y-TZP. The fracture strength of (4Y,4Ce)-TZP–Al_2O_3 composites increased from 1050 to 1800 MPa following hot isostatic pressing [15]. No monoclinic phase was detected by X-ray diffraction analysis in these as-sintered materials listed in Table II.

3.2. Stability of tetragonal zirconia

To estimate the stability of tetragonal zirconia, thermal and hydrothermal deterioration testing was conducted. Formation of m-ZrO_2 was investigated by X-ray diffraction analysis on the surface of sintered bodies. The results are shown in Figs 2 and 3. No monoclinic phase was detected by X-ray diffraction analysis on the surface of as-sintered test specimens, but a slight amount of m-ZrO_2 was formed on the surface of 3Y-TZP and (2.5Y,4Ce)-TZP by grinding using a 140 grit diamond wheel. For (4Y,4Ce)-TZP and (4Y,4Ce)-TZP–Al_2O_3 composites, no monoclinic layer was introduced by grinding with a diamond wheel as shown in Fig. 2a. After thermal ageing at 250 °C for 500 h, 3Y-TZP showed significant change in the crystalline phase. The fraction of monoclinic phase on the surface of 3Y-TZP increased. (2.5Y,4Ce)-TZP also showed a slight increase in monoclinic

TABLE II Bulk density, grain size of zirconia, bending strength and elastic modulus of TZP and TZP–Al_2O_3 composites

Material	Sintering temp. (°C)	Specimen	Bulk density (g cm^{-3})	Grain size (μm)	Bending strength (MPa)	Elastic modulus (GPa)
(2.5Y,4Ce)-TZP	1500	2.5Y4Ce	6.03	0.8	1000	–
(4Y,4Ce)-TZP	1500	4Y4Ce	6.05	0.6	840	195
3Y-TZP	1500	3Y	6.08	0.5	1050	217
(4Y,4Ce)-TZP–25 wt % Al_2O_3	1500	4Y4Ce25A	5.38	0.5	1050	255
	1400 HIP[a]	4Y4Ce25AH	5.39	0.35	1800	–
3Y-TZP–25 wt % Al_2O_3	1500	3Y25A	5.37	0.4	1100	255
	1400 HIP[a]	3Y25AH	5.38	0.3	2050	–

[a] Hot isostatic pressing in Ar gas.

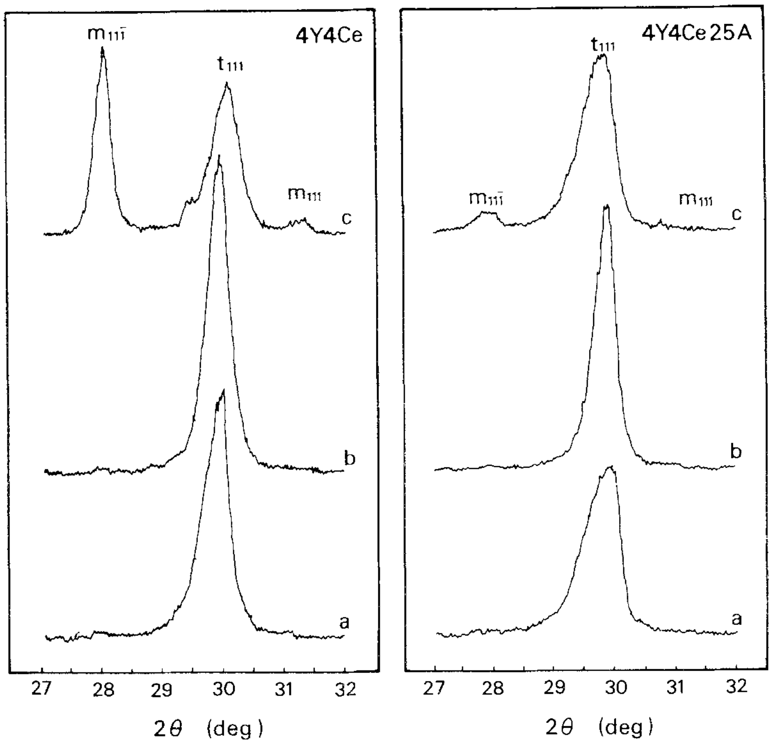

Figure 2 X-ray diffraction patterns on the surface of (4Y,4Ce)-TZP and (4Y,4Ce)-TZP–Al_2O_3 composites sintered at 1500 °C: (a) before ageing test (specimens ground using a 140 grit diamond wheel); (b) after thermal ageing at 250 °C for 500 h in air; (c) after hydrothermal ageing at 180 °C and 1 MPa for 35 h.

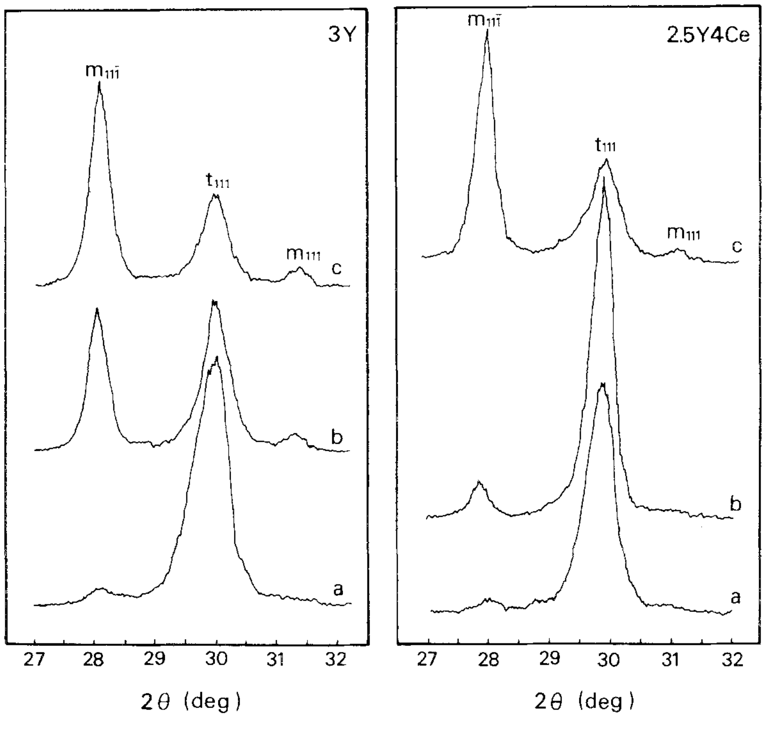

Figure 3 X-ray diffraction patterns on the surface of 3Y-TZP and (2.5Y,4Ce)-TZP sintered at 1500 °C: (a) before ageing test (specimens ground using a 140 grit diamond wheel); (b) after thermal ageing at 250 °C for 500 h in air; (c) after hydrothermal ageing at 180 °C and 1 MPa for 35 h.

phase, but the amount of m-ZrO_2 formed was smaller than that of 3Y-TZP.

(4Y,4Ce)-TZP and (4Y,4Ce)-TZP–Al_2O_3 composites showed no increase in monoclinic phase during 500 h ageing tests in air at 250 °C. After 35 h hydrothermal ageing tests at 180 °C and 1 MPa, metastable tetragonal phase on the surface of 3Y-TZP, (2.5Y,4Ce)-TZP and (4Y,4Ce)-TZP fully transformed to monoclinic phase. In contrast with these materials, formation of monoclinic phase on the surface of (4Y,4Ce)-TZP–Al_2O_3 composites was very slight. The amount of monoclinic phase after 10 h

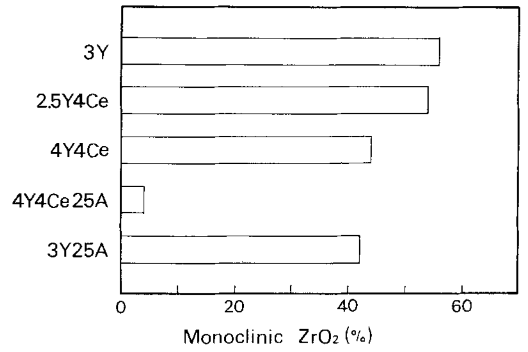

Figure 4 The amount of monoclinic phase of TZP and TZP–Al_2O_3 composites sintered at 1500 °C after 10 h hydrothermal ageing tests at 180 °C and 1 MPa.

hydrothermal ageing tests at 180 °C and 1 MPa is shown in Fig. 4. After 10 h hydrothermal ageing at 180 °C and 1 MPa, the increase of monoclinic phase on the surface of 3Y-TZP attained saturation.

It has been reported that hydrothermal ageing is more severe than thermal ageing in air, so that the t → m phase transformation is greatly accelerated by water [16]. (4Y,4Ce)-TZP (which was stable for thermal ageing at 250 °C) showed a significant increase of monoclinic phase during hydrothermal ageing at 180 °C and 1 MPa as shown in Fig. 2. This result gives evidence supporting that report in the present study. These results indicated that the tetragonal phase of (4Y,4Ce)-TZP–Al_2O_3 composites was more stable at lower temperatures in the presence of water than that of 3Y-TZP.

Fig. 5 shows the effect of alumina content in (Y,Ce)-TZP–Al_2O_3 composites on the resistance to phase transformation during hydrothermal ageing. From this result, the resistance to phase transformation under hydrothermal conditions was improved as the alumina content increased. It is noticeable that dispersing the alumina in both 3Y-TZP and (4Y,4Ce)-TZP is effective in resisting the t → m phase transformation. In (4Y,4Ce)-TZP–Al_2O_3 composites, dispersing 25 wt % Al_2O_3 could fully suppress the formation of monoclinic phase during 20 h hydrothermal ageing. In 3Y-TZP–Al_2O_3 composites, although dispersing the alumina was effective, it could not suppress the t → m phase transformation.

3.3. Changes in microstructure

Fig. 6 shows the microstructure of the surface of sintered bodies aged under hydrothermal condition at 180 °C and 1 MPa for 35 h. Many microcracks were observed on the surface of 3Y-TZP. As shown in Fig. 2, metastable tetragonal ZrO_2 phase on the surface of 3Y-TZP almost transformed to monoclinic structure after 10 h hydrothermal ageing. The phase transformation caused microcracks on the surface. (2.5Y, 4Ce)-TZP and (4Y,4Ce)-TZP also showed degradation, and microcracks were observed on the surface of sintered bodies after hydrothermal ageing. Especially in (Y,Ce)-TZP, the surface layer was peeled off by hydrothermal ageing for more than 15 h. In contrast with 3Y-TZP, (2.5Y,4Ce)-TZP and (4Y,4Ce)-TZP, changes in microstructure did not occur and microcracking was not observed on the surface of (4Y,4Ce)-TZP–Al_2O_3 composites as seen in Fig. 6.

Microstructures of the cut surface of the sintered bodies aged under hydrothermal condition at 180 °C and 1 MPa for 35 h are shown in Figs 7, 8 and 9. A transformed layer was clearly observed for 3Y-TZP and (2.5Y,4Ce)-TZP. As seen in Figs 7 and 8, the monoclinic phase of zirconia was formed on the surface and invaded the inside of the body accompanied by micropacks. The transformed layer depths for 3Y-TZP and (2.5Y,4Ce)-TZP were 150 and 380 μm, respectively. For (4Y,4Ce)-TZP–Al_2O_3 composites a transformed layer was not observed. (4Y,4Ce)-TZP–25 wt % Al_2O_3 composites showed no change in microstructure and were stable as compared with 3Y-TZP and (Y,Ce)-TZP during hydrothermal ageing for 35 h. From these comparisons, it is clear that the tetragonal phase of (4Y,4Ce)-TZP–25 wt % Al_2O_3 composites are highly resistant to phase transformation during ageing at low temperatures.

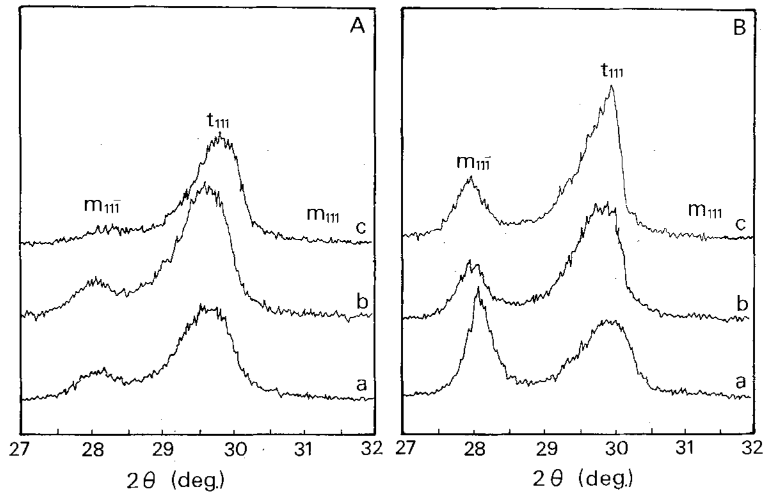

Figure 5 The effect of alumina content in (A) (4Y,4Ce)-TZP–Al_2O_3 and (B) 3Y-TZP–Al_2O_3 composites HIPed at 1400 °C on the resistance to tetragonal-to-monoclinic phase transformation during hydrothermal ageing at 180 °C and 1 MPa for 20 h: (a) 5 wt % Al_2O_3, (b) 12.5 wt % Al_2O_3, (c) 25 wt % Al_2O_3.

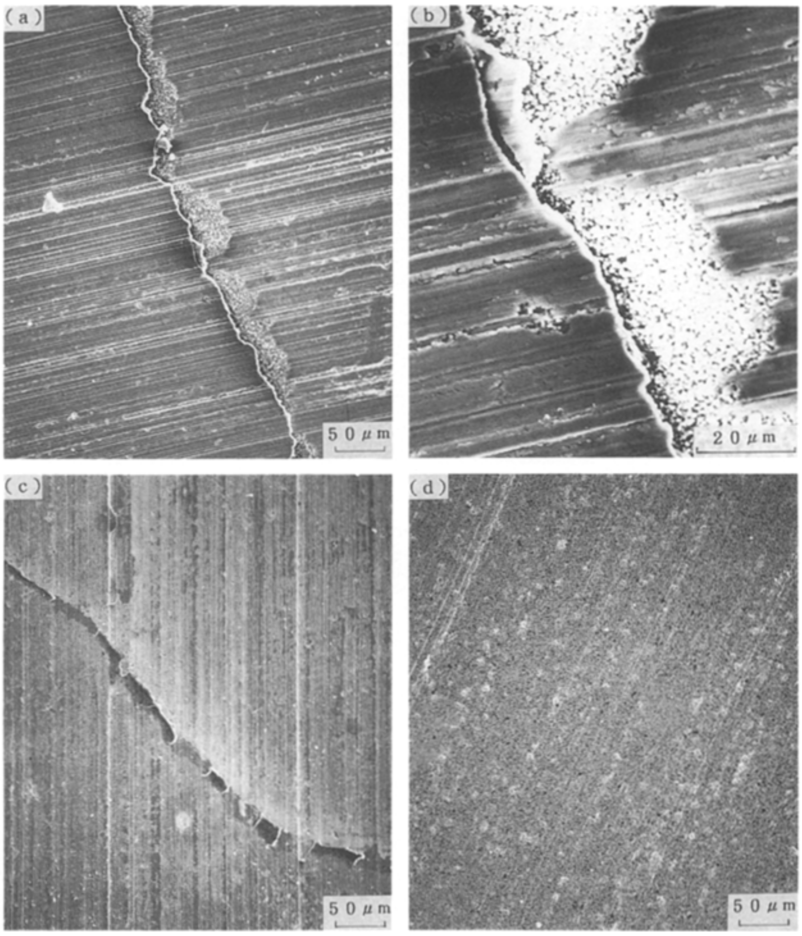

Figure 6 SEM photographs of the surface of sintered bodies after hydrothermal ageing at 180 °C and 1 MPa for 35 h: (a, b) 3Y-TZP sintered at 1500 °C; (c) (2.5Y,4Ce)-TZP sintered at 1500 °C; (d) (4Y,4Ce)-TZP–25 wt % Al_2O_3 composites sintered at 1500 °C.

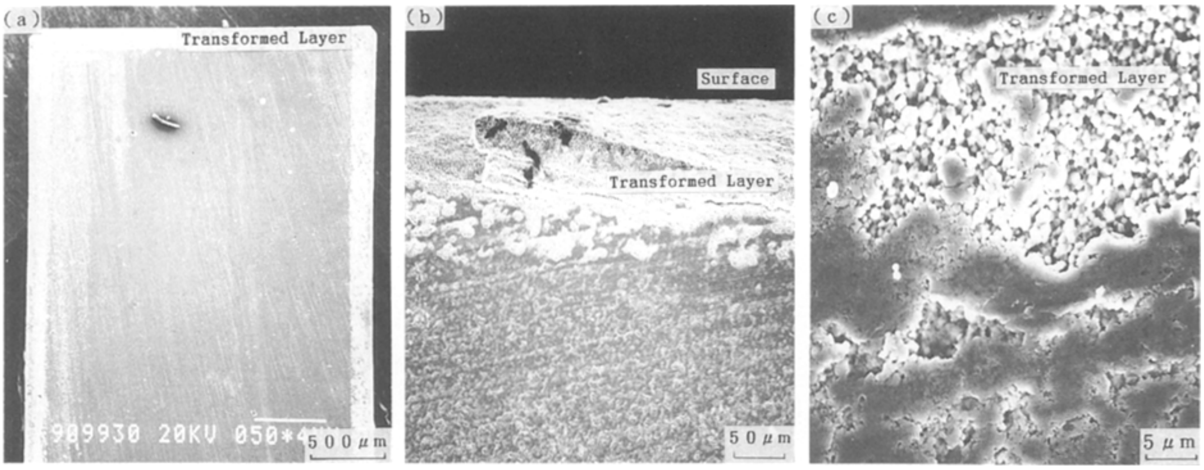

Figure 7 SEM photographs of the cut surface of 3Y-TZP sintered at 1500 °C after hydrothermal ageing at 180 °C and 1 MPa for 35 h: (a), (b) and (c) indicate the difference in microstructure between the transformed layer and the inside of the body.

4. Summary

(4Y,4Ce)-TZP was stable for atmospheric ageing at 250 °C, but monoclinic zirconia was formed on the surface and the transformation invaded the inside of the body accompanied by microcracks during hydrothermal ageing. Dispersion of Al_2O_3 into (Y,Ce)-TZP was useful to suppress the t → m phase transformation during hydrothermal ageing and to increase the fracture strength. (4Y,4Ce)-TZP–25 wt % Al_2O_3 composites were highly resistant to phase transformation during hydrothermal ageing.

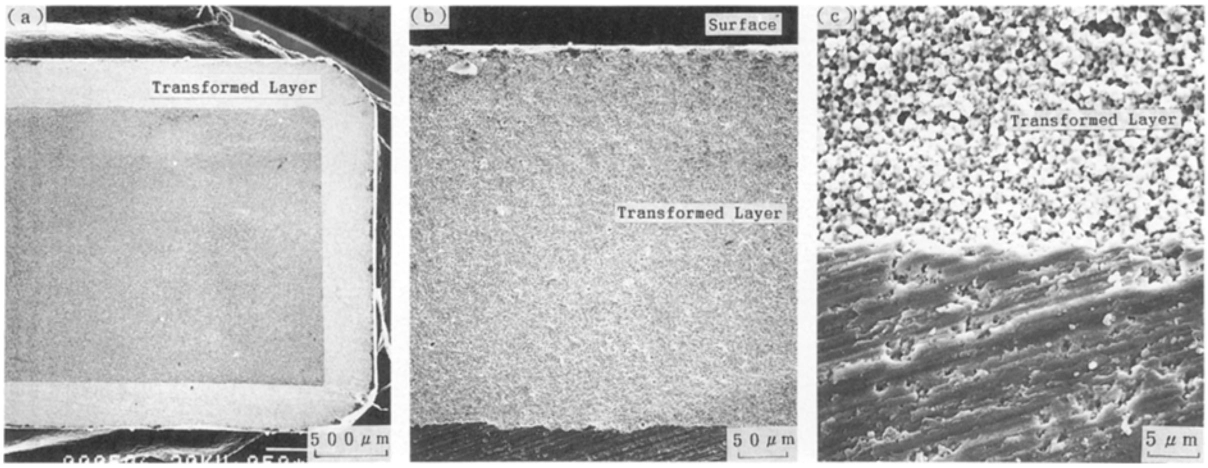

Figure 8 SEM photographs of the cut surface of (2.5Y,4Ce)-TZP sintered at 1500 °C after hydrothermal ageing at 180 °C and 1 MPa for 35 h: (a), (b) and (c) indicate the difference in microstructure between the transformed layer and the inside of the body.

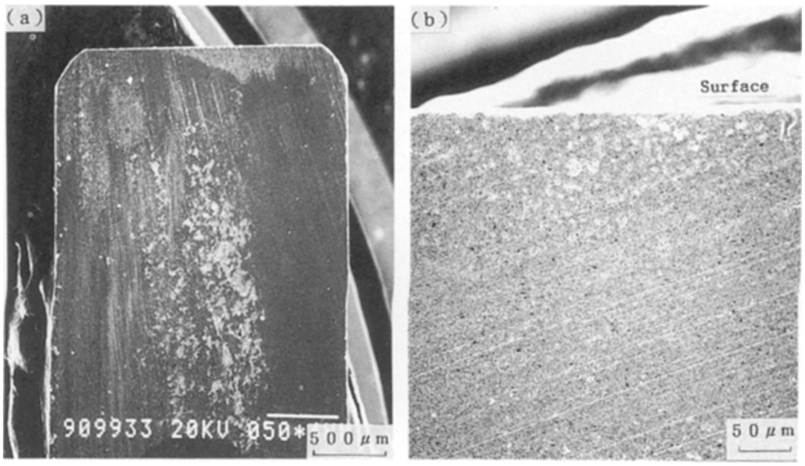

Figure 9 SEM photographs of the cut surface of (4Y,4Ce)-TZP–25 wt % Al_2O_3 composites sintered at 1500 °C after hydrothermal ageing at 180 °C and 1 MPa for 35 h: (a) and (b) indicate that no transformed layer is observed.

References

1. T. K. GUPTA, F. F. LANGE and J. H. BECHTOLD, *J. Mater. Sci.* **13** (1978) 1464.
2. F. F. LANGE, *ibid.* **17** (1982) 240.
3. K. KOBAYASHI, H. KUWAJIMA and T. MASAKI, *Solid State Ionics* (3–4) (1981) 489.
4. T. SATO and M. SHIMADA, *J. Amer. Ceram. Soc.* **67** (1984) c-212
5. *Idem, ibid.* **68** (1985) 356.
6. F. F. LANGE, G. L. DUNLOP and B. I. DAVIS, *ibid.* **69** (1986) 237.
7. P. J. WHALEN, F. REIDINGER and R. F. ANTRIM, *ibid.* **72** (1989) 319.
8. K. TSUKUMA, *Amer. Ceram. Soc. Bull.* **65** (1986) 1386.
9. T. SATO, T. FUKUSHIMA, T. ENDO and M. SHIMADA, in Proceedings of International Conference on the Science of Ceramics, vol. 14, pp. 843–48.
10. T. SATO, T. ENDO and M. SHIMADA, *J. Amer. Ceram. Soc.* **72** (1989) 761.
11. F. F. LANGE, *J. Mater. Sci.* **17** (1982) 247.
12. M. HIRANO and H. INADA, *J. Ceram. Soc. Jpn.* **99** (1991) 124.
13. R. C. GARVIE and P. S. NICHOLSON, *J. Amer. Ceram. Soc.* **55** (1972) 303.
14. K. URABE, K. OGATA, H. IKAWA and S. UDAGAWA, in Abstracts of American Ceramic Society 39th Pacific Coast Regional Meeting (1986) p. 45.
15. M. HIRANO, T. MATSUYAMA, H. INADA, K. SUZUKI, H. YOSHIDA and M. MACHIDA, *J. Ceram. Soc. Jpn.* **99** (1991) 395.
16. K. NAKAJIMA, K. KOBAYASHI and Y. MURATA, in "Advances in Ceramics", Vol. 12, edited by N. Claussen, M. Ruhle and A. H. Heuer (American Ceramic Society, Columbus, Ohio, 1984) pp. 399–407.

Received 18 July 1990
and accepted 6 February 1991